

1 APA-Scan: Detection and Visualization of 3'-UTR

2 Alternative Polyadenylation with RNA-seq and 3'-

3 end-seq Data

4 *Naima Ahmed Fahmi¹, Khandakar Tanvir Ahmed¹, Jae-Woong Chang³, Heba Nassereddeen²,*
5 *Deliang Fan⁴, Jeongsik Yong^{3†} and Wei Zhang^{1*†}*

6

7 * Correspondence: wzhang.cs@ucf.edu

8 ¹ Department of Computer Science, University of Central Florida, 4000 Central Florida Blvd,
9 Orlando, FL 32816, USA

10 Full list of author information is available at the end of the article

11 [†] Joint corresponding authors

12

13

Abstract

14 **Background** The eukaryotic genome is capable of producing multiple isoforms from a gene by
15 alternative polyadenylation (APA) during pre-mRNA processing. APA in the 3'-untranslated
16 region (3'-UTR) of mRNA produces transcripts with shorter or longer 3'-UTR. Often, 3'-UTR
17 serves as a binding platform for microRNAs and RNA-binding proteins, which affect the fate of
18 the mRNA transcript. Thus, 3'-UTR APA is known to modulate translation and provides a mean
19 to regulate gene expression at the post-transcriptional level. Current bioinformatics pipelines have
20 limited capability in profiling 3'-UTR APA events due to incomplete annotations and a low-
21 resolution analyzing power: widely available bioinformatics pipelines do not reference actionable
22 polyadenylation (cleavage) sites but simulate 3'-UTR APA only using RNA-seq read coverage,
23 causing false positive identifications. To overcome these limitations, we developed APA-Scan, a
24 robust program that identifies 3'-UTR APA events and visualizes the RNA-seq short-read
25 coverage with gene annotations.

26 **Methods** APA-Scan utilizes either predicted or experimentally validated actionable
27 polyadenylation signals as a reference for polyadenylation sites and calculates the quantity of long
28 and short 3'-UTR transcripts in the RNA-seq data. APA-Scan works in three major steps: (i)
29 calculate the read coverage of the 3'-UTR regions of genes; (ii) identify the potential APA sites
30 and evaluate the significance of the events among two biological conditions; (iii) graphical
31 representation of user specific event with 3'-UTR annotation and read coverage on the 3'-UTR
32 regions. APA-Scan is implemented in Python3. Source code and a comprehensive user's manual
33 are freely available at <https://github.com/combiolabucf/APA-Scan>.

34 **Result** APA-Scan was applied to both simulated and real RNA-seq datasets and compared with
35 two widely used baselines DaPars and APAtrap. In simulation APA-Scan significantly improved
36 the accuracy of 3'-UTR APA identification compared to the other baselines. The performance of
37 APA-Scan was also validated by 3'-end-seq data and qPCR on mouse embryonic fibroblast cells.
38 The experiments confirm that APA-Scan can detect unannotated 3'-UTR APA events and improve
39 genome annotation.

40 **Conclusion** APA-Scan is a comprehensive computational pipeline to detect transcriptome-wide
41 3'-UTR APA events. The pipeline integrates both RNA-seq and 3'-end-seq data information and
42 can efficiently identify the significant events with a high-resolution short reads coverage plots.

43 **Keywords** alternative polyadenylation; transcriptome; RNA-seq; 3'-end-seq

44

45

Introduction

46 Poly(A)-tails are added to pre-mRNA after the polyadenylation signal (PAS) during the 3'-
47 end processing of pre-mRNA [1]. The last exon of mRNA contains a non- coding region, 3'-
48 untranslated region (3'-UTR), which spans from the termination codon to the polyadenylation site.
49 The 3'-UTR acts as a molecular scaffold to bind microRNAs and RNA-binding proteins and
50 functions in regulatory gene expression [2]. In human and mouse, more than 70% of genes contain
51 multiple PASs in their 3'- UTRs and polyadenylation using upstream PASs leads to the production
52 of mRNA with shortened 3'-UTRs (3'-UTR APA) [3, 4]. 3'-UTR APA is known to increase the
53 efficiency of translation and is associated with T cell activation, oncogene activation, and poor
54 prognosis in many diseases [5, 6, 7]. Recent study has demonstrated that 3'- UTR APA is one way
55 to increase protein synthesis without increasing the quantities of mRNAs, indicating that it is an
56 important element in gene expression which cannot be understood by conventional differential
57 gene or transcript expression analysis [8]. Up-regulation of mTOR signaling pathway can lead to
58 transcriptome- wide 3'-UTR APA [8, 9].

59 3'-UTR APA has gained much attention recently and the importance of the 3'- UTR APA
60 in human diseases has been demonstrated as mentioned above. Some recent studies show that both
61 proliferating cells and transformed cells favor expression of shorter 3'-UTR through APA and lead
62 to the activation of oncogenes [6, 10]. Some other research shows the trend in cancer cells for
63 highly expressed genes to exhibit shorter 3'-UTR with fewer microRNA binding sites, decreasing
64 microRNA- mediated translation repression [5, 11]. All these studies imply that 3'-UTR APA may
65 serve as a new layer of prognostic biomarker. A scalable computational model is highly needed to
66 detect the genome-wide unannotated 3'-UTR APA in different phenotypes.

67 Several bioinformatics pipelines are available for the analysis of UTR-APA using RNA-
68 seq data [12, 13, 14, 15, 16]. In general, all these methods measure the changes in 3'-UTR lengths
69 by modeling the RNA-seq read density change near the 3'-end of mRNAs. Indeed, with the aid of
70 these methods, RNA-seq experiments became a powerful approach to investigate 3'-UTR APA.
71 However, in many cases the identified APA sites are not functionally and physiologically relevant
72 because most pipelines do not reference actionable PASs in their 3'-UTR APA simulation. RNA-
73 seq is not particularly accurate when it comes to identifying polyadenylation sites, making novel
74 APA transcript identification rather difficult. Therefore, 3'-end- seq data has been developed to

75 address these issues by enriching for 3'-end reads in high-throughput sequencing experiment [17]
76 and provides the accurate polyadenylation sites. In addition to the limitations of the current
77 bioinformatics pipelines mentioned above, none of them can provide high-resolution read
78 coverage plots of the APA events with an accurate annotation. We have developed APA-Scan
79 (Figure 1), a bioinformatics program, to detect and visualize genome-wide 3'-UTR APA events.
80 APA-Scan integrates both 3'-end-seq data and the location information of predicted canonical
81 PAs with RNA-seq data to improve the quantitative definition of genome-wide UTR APA events.
82 APA-Scan efficiently manages large-scale alignment files and generates a comprehensive analysis
83 for UTR APA events. It is also advantageous in producing high quality plots of the events.

84

85 **Results**

86 APA-Scan is designed to identify both annotated and de novo 3'-UTR APA events between
87 different biological conditions. To access the performance of APA-Scan, it was compared with
88 two baseline methods on both simulated and real RNA-seq datasets. In the simulation experiment,
89 we first generated synthetic dataset with pre-defined 3'-UTR APA events (ground truth) to test if
90 the APA-Scan and baseline methods can detect them. Next, we performed experiments on two
91 mouse embryonic fibroblast (MEF) cells to evaluate the performance of APA-Scan. The results of
92 analyzing real MEF RNA-seq datasets were validated using both qPCR and 3'-end-seq data.

93 **Experimental results with simulated RNA-seq data**

94 In the simulation experiment, we generated synthetic RNA-seq short reads with flux-
95 simulator [18]. 1000 pre-defined 3'-UTR APA events were simulated as the ground truth between
96 two different conditions. In each condition, three technical replicates were generated by repeating
97 the experiment three times with the same parameter setting in the flux simulator. The details of the
98 parameters used in this experiment are provided in the Additional file 2. For both conditions, the
99 gene expressions were sampled from a Poisson distribution to reflect a real RNA-seq data [19].
100 For each gene, one proximal polyadenylation site was synthesized to represent the end of the short
101 isoform and the end of the annotated transcript was applied to define the end of the long isoform
102 of that gene. To generate the ground truth profile of the 3'-UTR APA events, the expression
103 proportions of the short and long isoforms in the same gene were assigned significantly different

104 values in two conditions (i.e., the proportion difference was larger than 10%) to represent the
105 existence of the APA event.

106 In the simulation experiment, two sets of synthetic data were generated by flux- simulator.
107 One with 30M (30 million) paired-end reads in each replicate and one with 50M paired-end read.
108 In both cases, the read length is 76 bps of each end. APA-Scan was compared with DaPars and
109 APAtrap on the simulated RNA-seq datasets. To detect the significant 3'-UTR APA events, APA-
110 Scan used p -value < 0.05 (χ^2 -test) as the cutoff. DaPars identified APA events according to the
111 difference in PDUI (Percentage of Distal polyA Usage Index) values between two conditions $>$
112 0.1 and FDR < 0.05 ; whereas APAtrap selected events using the cutoff values of two parameters:
113 percentage difference of APA site usage between two conditions > 0.1 and FDR < 0.05 . The
114 performance of the methods is then evaluated using AUC score, sensitivity and specificity. Figure
115 2 shows that, APA-Scan outperformed the two baselines in terms of AUC scores and got the best
116 score of 0.94 in both sequence depths (30M reads and 50M reads) and followed by APAtrap (0.73
117 in 30 million reads case and 0.75 in 50 million reads case). DaPars did not work very well
118 compared to the other two methods and the AUC scores were below 0.7 in both cases, though there
119 was an improvement in the case with more reads. We also report the sensitivity and specificity for
120 each method with two different sequencing depths in Table 2. APA-Scan gets the highest
121 sensitivity and specificity scores for both cases, which indicates that APA-Scan outperformed the
122 baseline methods in detecting the true 3'-UTR APA events and eliminating the true negative ones.

123 As different sequencing depths may affect the performance of APA-Scan, we generated
124 five simulation experiments with different read depths, i.e., 2M, 5M, 10M, 30M, and 50M paired-
125 end reads by flux-simulator with the same parameter setting to learn the impact of sequencing
126 depths in the analysis of 3'-UTR APA with APA- Scan. In this experiment, the read length was
127 also 76 bps for each end and three replicates were generated for each condition in each read depth
128 using the same procedures as mentioned in the previous section. Figure 3 shows the ROC curves
129 for different sequencing depth on detecting the 3'-UTR APA events. APA-Scan shows moderate
130 performance with low sequencing depths (i.e., 2M and 5M). However, the performance of APA-
131 Scan improved drastically (AUC = 0.94) after it reached to a certain sequencing depth (i.e., 10M
132 in this study) and holds that performance across read depths above that threshold. This result

133 suggests that APA-Scan is quite robust in detecting APA events on lowly expressed genes and
134 relatively low read coverage samples.

135 **Experimental results with MEFs samples**

136 In the real RNA-seq experiments, two MEFs samples $Tsc1^{-/-}$ and WT were used in the
137 analysis to evaluate the performance of APA-Scan and baseline methods. Knockout of $Tsc1$, a
138 negative regulator of mTOR pathway, leads to uncontrolled mTOR hyper-activation compared
139 with WT. For the comparison and evaluation purposes, the APA-Scan was run on two different
140 setups. One used PAs in the 3'-UTRs as potential cleavage sites, and we denote it by APA-
141 Scan^{PAS}. The other one considered 3'-end-seq peaks as candidate sites, and it is denoted as APA-
142 Scan^{peaks}. First, APA-Scan^{PAS} was applied to detect 3'-UTR APA events between the two MEFs
143 samples with p-value < 0.05. APA-Scan^{PAS} detected 265 events, whereas DaPars and APAtrap
144 detected 785 and 1130 significant events, respectively. These events were then verified by the
145 polyadenylation sites reported by 3'-end-seq data. If a predicted 3'-UTR APA event is within 50
146 bps upstream or downstream of the loci of the peak(s) in 3'-end-seq data, then this APA event is
147 considered overlapping with the 3'-end-seq signals. Though APA-Scan^{PAS} detected less number
148 of significant events compared to the baseline methods, 87.92% (233) of the events were validated
149 by the 3'-end-seq signals according to the result shown in Figure 4 and Table 3. DaPars and
150 APAtrap identified more events than APA-Scan^{PAS}, however, both the number and ratio of the
151 overlapping events with the 3'-end-seq signals are significantly lower than the events detected by
152 APA-Scan^{PAS}. Note that APA-Scan^{PAS} did not use any information from 3'-end-seq data to identify
153 the APA events. These results concur with our findings in the simulation experiment that APA-
154 Scan not only do better detection on the true APA events but also prevent the false positives. Figure
155 5 shows the number of overlapped genes with the 3'-UTR APA events detected by the three
156 methods. From the results, we can conclude that the agreement of the three methods is not high
157 and most identified events were only detected by one method.

158 To further validate the analysis results by APA-Scan, we conducted qPCR experiments for
159 Srsf3 and Rpl22 transcripts from $Tsc1^{-/-}$ and WT MEFs based on the significant 3'-UTR APA
160 events reported by APA-Scan^{peaks}. These genes were selected due to the design of PCR
161 (polymerase chain reaction) primers for wet-lab validation. As shown in Figure 6, both Srsf3 and
162 Rpl22 showed the increase of the short 3'-UTR transcript by APA in $Tsc1^{-/-}$ compared to WT

163 MEFs, which is consistent with our observations on the RNA-seq and 3'-end-seq read coverage
164 plots. These results further confirm that APA-Scan can identify the true 3'-UTR APA events with
165 RNA-seq and 3'-end-seq samples from two different biological contexts. The more details of the
166 qPCR analysis and the primer sequences of the two genes are available in the Additional file 1.

167 Generally, the nucleotide profiles surrounding the polyadenylation sites are dominated by
168 two motifs and their variants: AATAAA and ATTAAA and these two hexamers are observed
169 upstream of the cleavage sites [20]. This phenomenon leads us to explore the nucleotide
170 composition near the predicted polyadenylation sites by APA-Scan^{peaks}. Figure 7 shows a high
171 concentration/cluster of nucleotide ‘A’ in the polyadenylation site, positioned at 0. The upstream
172 surrounding region is also dominated by ‘A’ and ‘T’, which clearly indicates the existence of
173 potential 3'-UTR APA events.

174

175 **Discussion**

176 APA is one mechanism for post-transcriptional regulation of mRNA expression, and it is
177 defined as use of more than one polyadenylation sites. 3'-UTR APA is one of the most frequent
178 APA forms, which contains more than one polyadenylation sites in the 3'-UTR. It generates
179 multiple mRNA transcripts with different 3'-UTR lengths without affecting the protein encoded
180 by the gene. Since the 3'-UTR of mRNA of- ten contains binding sites for microRNAs, 3'-UTR
181 APA potentially leads to altered mRNA stability or protein translation efficiency due to variation
182 of 3'-UTR length. Identification and assessment of APA sites has been a major goal in
183 understanding transcriptomic diversity. Several bioinformatics tools have been developed to
184 predict transcriptome-wide polyadenylation sites with RNA-seq data. However, our experimental
185 results on simulated and real samples indicate that the current methods (e.g., DaPars and APAtrap)
186 can detect large number of APA events, but significant portion of the events are false positives. A
187 similar data analysis on BT549 breast cancer cells (mock vs. torin 1 treated) in Figure S1 in the
188 Additional file 1 illustrates a similar pattern. By integrating 3'-end-seq and RNA-seq data, APA-
189 Scan can potentially reduce the number of false positive events. To evaluate the performance of
190 APA-Scan on real cancer patient samples, one pair (tumor vs. matched normal tissue) of The
191 Cancer Genome Atlas (TCGA) breast cancer samples are also analyzed and reported in the

192 Additional file 1. Figure S2 shows that a significant portion (>72%) of the 3'-UTR APA events
193 are not differentially expressed. There- fore, APA-based molecular signatures could provide
194 additional predictive power of cancer outcomes by combining the differently expressed genes.

195 APA-Scan not only can accurately detect the splicing events compared to the baseline
196 methods, but also provides reasonable running time. Table 4 shows a com- parison of the CPU
197 time of each method on $Tsc1^{-/-}$ and WT MEFs. The CPU time was measured on an Intel(R)
198 Xeon(R) CPU E5-2620 v4 @ 2.10GHz machine. Both APA-Scan and APAtrap completed the
199 analysis in a similar amount of time. However, DaPars is much slower than the other two methods
200 which is not suit- able to be applied on large-scale experiment in terms of running time. Overall,
201 this study reports an efficient and precise framework for 3'-UTR APA identification with RNA-
202 seq and 3'-end-seq data.

203

204 Conclusion

205 We developed APA-Scan, which offers a comprehensive computational pipeline to identify
206 transcriptome-wide 3'-UTR APA events. By integrating RNA-seq data and 3'-end-seq
207 information (experimentally verified or computationally predicted). APA-Scan can efficiently
208 identify significant APA events and also, can illustrate the events with read coverage plots. 3'-
209 end-seq signals and the wet-lab experiment using qPCR demonstrate that APA-Scan provides
210 high-accuracy and quantitative profiling of 3'-UTR APA events. Therefore, we expect that, APA-
211 Scan will serve as a useful tool for APA site analysis.

212

213 Methods

214 APA-Scan pipeline

215 APA-Scan workflow comprises of three major steps: (i) read coverage estimation; (ii)
216 identification of polyadenylation sites and the calculation of APA; (iii) graphical illustration of
217 UTR APA events (Figure 1). First, APA-Scan takes aligned RNA- seq and 3'-end-seq data from
218 two different biological conditions as input. Each biological condition can have multiples samples

219 or replicates. The read coverage files are generated by SAMtools [21]. In this step, the 3'-end-seq
220 data is an optional input.

221 In the second step, APA-Scan starts the analysis by extracting 3'-UTR frames for each
222 gene. APA-Scan is designed in two modes: (a) Default, and (b) Extended. All the aligned reads
223 from 3'-end-seq data are pooled together to identify peaks and the corresponding unannotated
224 cleavage sites in 3'-UTR regions and downstream of the 3'-UTR regions (i.e., APA-Scan^{peaks}). In
225 the Default mode, 3'-UTR regions are selected according to the end of the longest annotated
226 transcript of the gene. The loci of peaks identified in the 3'-end-seq data are considered as potential
227 cleavage sites. If the 3'-end-seq data is not provided by the user, detected PASs (generally two
228 variations of the hexamers: AATAAA, ATTAAA) in 3'-UTRs are considered as the potential
229 cleavage sites (i.e., APA-Scan^{PAS}) follow the ideas in Omni-PolyA [16] which use 12 most
230 common PAS variants to determine the cleavage sites. In the Extended mode of APA-Scan, the
231 potential peaks/PAS signals are searched up to 10kb downstream of the end of transcript to
232 discover de novo distal polyadenylation sites. The locations detected from all input samples are
233 merged to get a combined list of potential cleavage sites. The major commands and general
234 terminologies to run APA-Scan are listed in Table 1.

235 APA-Scan evaluates each empirical cleavage site in the 3'-UTR of a transcript by
236 contrasting the RNA-seq short reads coverage up and downstream of the candidate site between
237 the two biological conditions. n and N denote the average read coverage up and downstream of
238 the site. They are determined by estimating the number of reads mapped to upstream and
239 downstream of the cleavage site, r_u and r_d , divided by their effective length, l_u and l_d , respectively
240 (i.e., $n = \frac{r_u}{l_u}$ and $N = \frac{r_d}{l_d}$). For each potential polyadenylation site, the ratio differences between the
241 samples in two conditions are calculated based on the following equation

$$\frac{n_1}{N_1} - \frac{n_2}{N_2},$$

242
243 where 1 and 2 represent the two conditions. Ratio difference indicates the change in read coverage
244 between two conditions and only the absolute ratio difference > 0.1 is considered as candidate site
245 for the further analysis. After that, the canonical $2 \times 2 \chi^2$ -test is applied to report the p-value for
246 each candidate site. The χ^2 -test measures how much the observation deviates from the null
247

248 hypothesis. In our experiment, we set the null hypothesis as the average read coverage before and
249 after the cleavage sites are consistent among the two biological conditions. For any true 3'-UTR
250 APA event, there must be a significant read coverage drop-off around the cleavage sites, and the
251 ratios of the average read coverages before and after the cleavage sites are crucially different in
252 the two conditions. In such cases, the χ^2 -test precisely reports significant p-values to reject our
253 null hypothesis. APA-Scan will report both significant and insignificant in an Excel file. A
254 comprehensive user's manual is provided in the Additional file 2.

255 In the third step, based on the significance of 3'-UTR APA events calculated in the previous
256 step, APA-Scan generates RNA-seq and 3'-end-seq (if provided) read coverage plots with the 3'-
257 UTR annotations for one or more user-specific events. Users may specify the region of the genome
258 locus to generate the read alignment plot. Figure 1 (Step 3) illustrates an example of the read
259 coverage plot generated by APA-Scan.

260 **Baselines and evaluation methods**

261 In this study, two widely used 3'-UTR APA identification approaches, DaPars [12] and
262 APAtrap [15] were applied to compare the performance with APA-Scan. The command lines to
263 run the baseline methods are available in the Additional file 1. To evaluate the performance of
264 APA-Scan and baseline methods, the area under the ROC curve (AUC), sensitivity and specificity
265 were used on the identified lists of 3'-UTR APA events.

266 **Short read alignments and peak identification**

267 In this study, two mouse embryonic fibroblasts (MEFs) samples and two breast cancer cell
268 lines (BT549) were used in the analysis to evaluate the performance of APA-Scan and baseline
269 methods. For the MEFs samples, we performed RNA- seq and 3'-end-seq analyses of poly(A+)
270 RNAs isolated from $Tsc1^{-/-}$ and wild- type (WT) MEFs. In the RNA-seq analysis, 63,742,790
271 paired-end reads for WT and 74,251,891 paired-end reads for $Tsc1^{-/-}$ MEFs were produced from
272 Hi-Seq pipeline with length of 50 bps of each end. The short reads were aligned to the mm10
273 reference genome by TopHat2 [22], allowing up to two mismatches. Finally, 87.1% of short reads
274 from WT and 87.5% of sequence reads from $Tsc1^{-/-}$ MEFs were mapped to the reference genome
275 for APA analysis in the study. In the 3'-end- seq analysis, the reads from WT and $Tsc1^{-/-}$ MEFs
276 were preprocessed to trim A's off the 3'-ends and then filtered by removing the reads of low-

277 quality 3'-end (Phred score < 30) and shorter than 25 bps. The remaining reads were aligned to the
278 mm10 reference genome by Bowtie [23] without allowing any mismatches. In total, 6,186,893
279 paired-end reads were aligned for WT and 5,382,111 reads were aligned for *Tsc1*^{-/-}. All aligned
280 reads from 3'-end-seq were pooled together in order to identify peaks and the corresponding
281 cleavage sites in the reference genome by the read coverage signals. In each read alignment 'hill',
282 the location with the highest read coverage between two zero coverage positions was considered
283 as the peak of the 'hill'. The 3'-end of the peak is chosen as the potential corresponding cleavage
284 sites where the read coverage at the peak quantifies the cleavage at the site. For the breast cancer
285 cell lines, we performed RNA-seq analysis of poly(A+) RNAs isolated from BT549 mock and
286 Torin1 treated cells. 131,955,082 paired-end reads for BT549 mock, and 138,127,113 paired-end
287 reads for BT549 treated with Torin1 were produced from Hi-Seq pipeline with length of 51 bps of
288 each end. The short reads were aligned to the hg38 reference genome by TopHat2, allowing up to
289 two mismatches. Finally, 85.2% of short reads from BT549 mock and 84.7% of sequence reads
290 from BT549 treated with Torin1 were mapped to the reference genome for APA analysis in the
291 study.

292

293 **Declarations**

294 **Abbreviations**

295 APA: alternative polyadenylation 3'-UTR: 3'-untranslated region

296 mTOR: mechanistic target of rapamycin PAS: polyadenylation signal

297 MEFs: mouse embryonic fibroblasts WT: wild-type

298 ROC: receiver operating characteristic AUC: area under the ROC curve

299 qPCR: quantitative polymerase chain reaction

300 **Ethics approval and consent to participate**

301 Not applicable.

302 **Consent for publication**

303 Not applicable.

304 **Availability of data and materials**

305 The source code in this study is available at: <https://github.com/combiolabucf/APA-Scan>. The
306 accession number for the MEFs RNA-seq data in this study is [SRP056624](#). The accession number
307 for the 3'-end-seq data in this study is [SRP133833](#).

308 **Competing interests**

309 The authors declare that they have no competing interests.

310 **Funding**

311 The study was supported by the National Science Foundation grant FET2003749 and National
312 Institutes of Health 1R01GM113952-01A1 and DK097771. Publication costs are funded by the
313 National Science Foundation grant FET2003749. The funding bodies had no role in study design,
314 data collection, data analysis and interpretation of data and in writing the manuscript.

315 **Author's contributions**

316 NAF, DF, JY, and WZ conceived the study and planned the analysis. NAF, KTA, and HN
317 performed data analysis. JWC and JY designed and performed qPCR experiments. NAF, KTA,
318 JY, and WZ wrote the manuscript. All authors read and approved the final manuscript.

319 **Author details**

320 ¹ Department of Computer Science, University of Central Florida, 4000 Central Florida Blvd,
321 Orlando, FL 32816, USA.

322 ² Department of Computer Engineering, University of Central Florida, 4000 Central Florida Blvd,
323 Orlando, FL 32816, USA.

324 ³ Department of Biochemistry, Molecular Biology and Biophysics, University of Minnesota Twin
325 Cities, 420 Washington Ave. S.E., Minneapolis, MN 55455, USA.

326 ⁴ School of Electrical, Computer and Energy Engineering, Arizona State University, 650 E Tyler
327 Mall, Tempe, AZ 85287, USA.

328

329

References

1. Proudfoot, N.J.: Ending the message: poly (A) signals then and now. *Genes & development* 25(17), 1770–1782 (2011)
2. Tian, B., Manley, J.L.: Alternative cleavage and polyadenylation: the long and short of it. *Trends in Biochemical Sciences* 38(6), 312–320 (2013)
3. Elkon, R., Ugalde, A.P., Agami, R.: Alternative cleavage and polyadenylation: extent, regulation and function. *Nature Reviews Genetics* 14(7), 496 (2013)
4. Yeh, H.-S., Zhang, W., Yong, J.: Analyses of alternative polyadenylation: from old school biochemistry to high-throughput technologies. *BMB reports* 50(4), 201 (2017)
5. Mayr, C., Bartel, D.P.: Widespread shortening of 3' UTRs by alternative cleavage and polyadenylation activates oncogenes in cancer cells. *Cell* 138(4), 673–684 (2009)
6. Lembo, A., Di Cunto, F., Provero, P.: Shortening of 3 UTRs correlates with poor prognosis in breast and lung cancer. *PloS one* 7(2), 31129 (2012)
7. Morris, A.R., Bos, A., Diosdado, B., Rooijers, K., Elkon, R., Bolijn, A.S., Carvalho, B., Meijer, G.A., Agami, R.: Alternative cleavage and polyadenylation during colorectal cancer development. *Clinical Cancer Research* 18(19), 5256–5266 (2012)
8. Chang, J.-W., Zhang, W., Yeh, H.-S., De Jong, E.P., Jun, S., Kim, K.-H., Bae, S.S., Beckman, K., Hwang, T.H., Kim, K.-S., et al.: mRNA 3-UTR shortening is a molecular signature of mTORC1 activation. *Nature communications* 6(1), 1–9 (2015)
9. Chang, J.-W., Zhang, W., Yeh, H.-S., Park, M., Yao, C., Shi, Y., Kuang, R., Yong, J.: An integrative model for alternative polyadenylation, IntMAP, delineates mTOR-modulated endoplasmic reticulum stress response. *Nucleic Acids Research* 46(12), 5996–6008 (2018)
10. Hoffman, Y., Bublik, D.R., P. Ugalde, A., Elkon, R., Biniashvili, T., Agami, R., Oren, M., Pilpel, Y.: 3'UTR shortening potentiates microRNA-based repression of pro-differentiation genes in proliferating human cells. *PLoS genetics* 12(2), 1005879 (2016)
11. Sandberg, R., Neilson, J.R., Sarma, A., Sharp, P.A., Burge, C.B.: Proliferating cells express mRNAs with shortened 3'untranslated regions and fewer microRNA target sites. *Science* 320(5883), 1643–1647 (2008)
12. Xia, Z., Donehower, L.A., Cooper, T.A., Neilson, J.R., Wheeler, D.A., Wagner, E.J., Li, W.: Dynamic Analyses of Alternative Polyadenylation from RNA-Seq Reveal 3'-UTR Landscape Across 7 Tumor Types. *Nature Communications* 5, 5274 (2014)

360 13. Wang, W., Wei, Z., Li, H.: A change-point model for identifying 3' UTR switching by next-
361 generation RNA sequencing. *Bioinformatics* 30(15), 2162–2170 (2014)

362 14. Le Pera, L., Mazzapioda, M., Tramontano, A.: 3USS: a web server for detecting alternative 3'
363 UTRs from RNA-seq experiments. *Bioinformatics* 31(11), 1845–1847 (2015)

364 15. Ye, C., Long, Y., Ji, G., Li, Q.Q., Wu, X.: APATrap: identification and quantification of
365 alternative polyadenylation sites from RNA-seq data. *Bioinformatics* 34(11), 1841–1849
366 (2018)

367 16. Magana-Mora, A., Kalkatawi, M., Bajic, V.B.: Omni-PolyA: a method and tool for accurate
368 recognition of Poly(A) signals in human genomic DNA. *BMC genomics* 18(1), 1–13 (2017)

369 17. Shepard, P.J., Choi, E.-A., Lu, J., Flanagan, L.A., Hertel, K.J., Shi, Y.: Complex and dynamic
370 landscape of rna polyadenylation revealed by pas-seq. *Rna* 17(4), 761–772 (2011)

371 18. Griebel, T., Zacher, B., Ribeca, P., Raineri, E., Lacroix, V., Guig'o, R., Sammeth, M.:
372 Modelling and simulating generic RNA-Seq experiments with the flux simulator. *Nucleic acids
373 research* 40(20), 10073–10083 (2012)

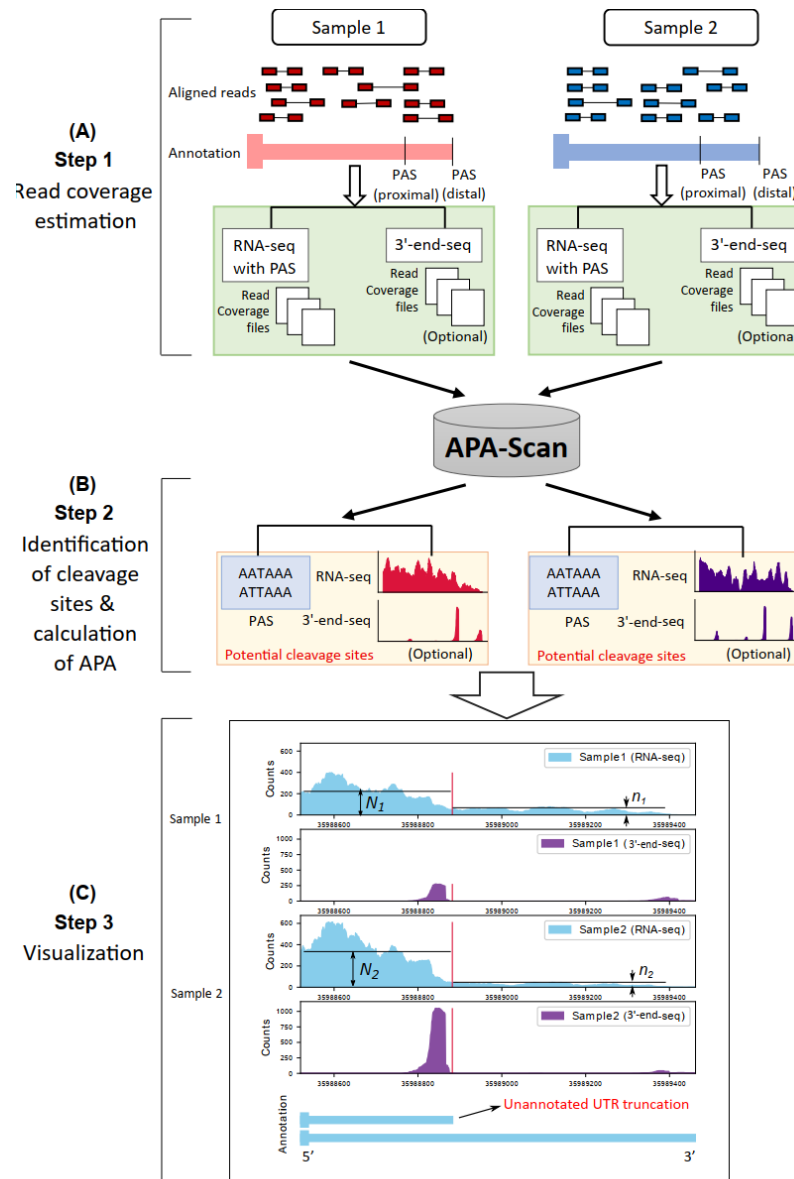
374 19. Oshlack, A., Robinson, M.D., Young, M.D.: From RNA-seq reads to differential expression
375 results. *Genome biology* 11(12), 220 (2010)

376 20. Gruber, A.J., Schmidt, R., Gruber, A.R., Martin, G., Ghosh, S., Belmadani, M., Keller, W.,
377 Zavolan, M.: A comprehensive analysis of 3 end sequencing data sets reveals novel
378 polyadenylation signals and the repressive role of heterogeneous ribonucleoprotein C on
379 cleavage and polyadenylation. *Genome research* 26(8), 1145–1159 (2016)

380 21. Li, H., Handsaker, B., Wysoker, A., Fennell, T., Ruan, J., Homer, N., Marth, G., Abecasis, G.,
381 Durbin, R.: The sequence alignment/map format and SAMtools. *Bioinformatics* 25(16), 2078–
382 2079 (2009)

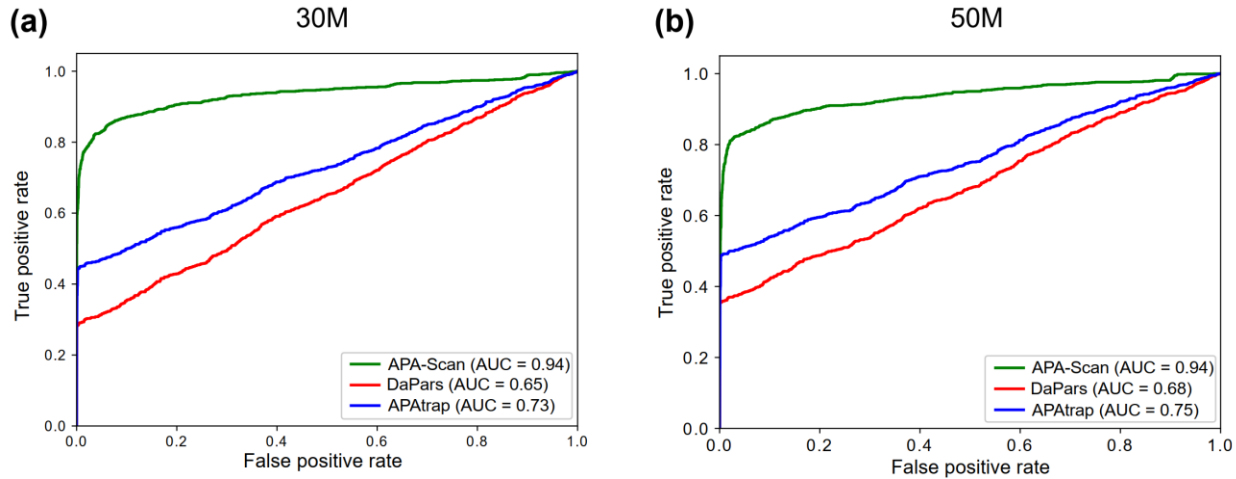
383 22. Kim, D., Pertea, G., Trapnell, C., Pimentel, H., Kelley, R., Salzberg, S.L.: TopHat2: accurate
384 alignment of transcriptomes in the presence of insertions, deletions and gene fusions. *Genome
385 biology* 14(4), 1–13 (2013)

386 23. Langmead, B., Trapnell, C., Pop, M., Salzberg, S.L.: Ultrafast and memory-efficient alignment
387 of short DNA sequences to the human genome. *Genome biology* 10(3), 1–10 (2009)



389

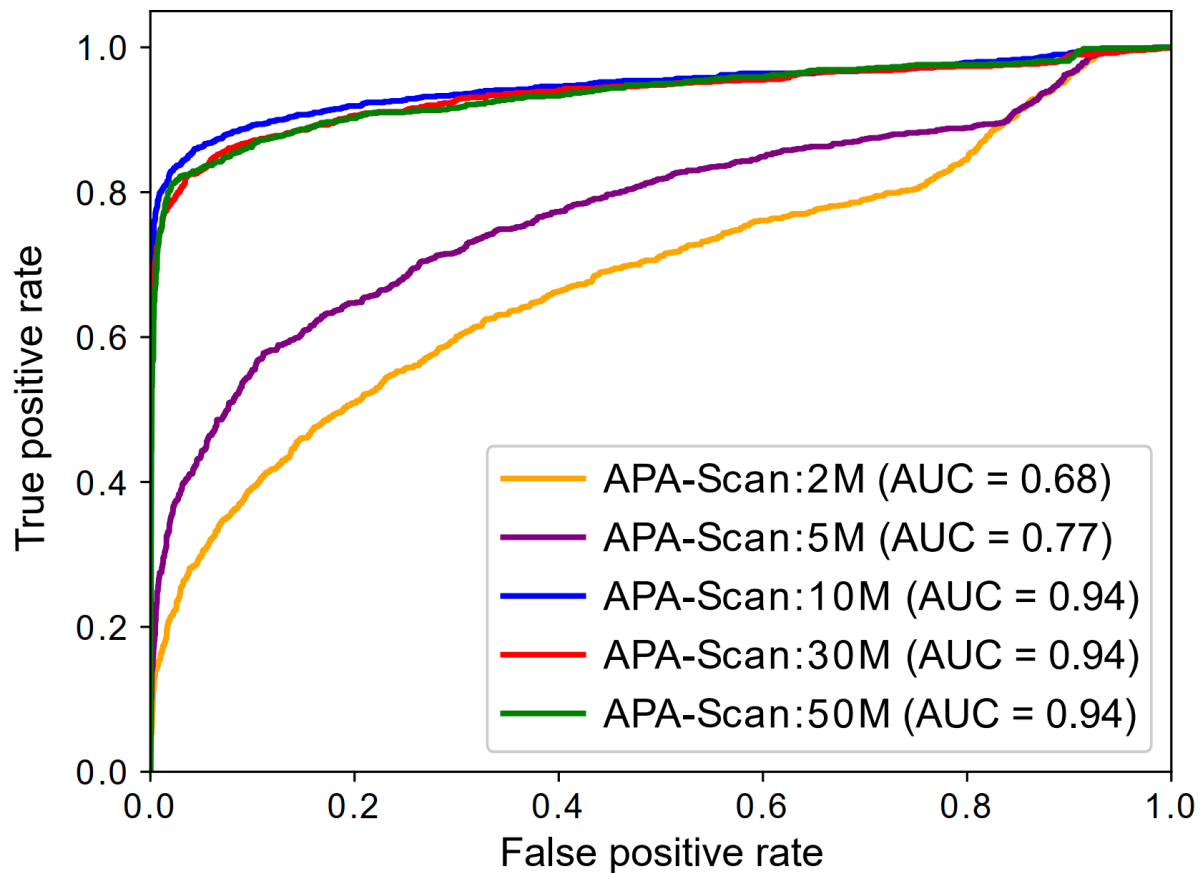
390 **Figure 1.** Workflow of APA-Scan. Starting with aligned RNA-seq and 3'-end-seq (optional)
391 bam files, APA-Scan consists of three steps and generates high quality graphical illustration of
392 aligned sequences with the indication of 3'-UTR APA events. (A) Read coverage files are
393 generated for RNA-seq and 3'-end-seq (if provided) input samples. (B) APA-Scan identifies
394 potential cleavage sites according to polyadenylation signal (PAS) hexamer: ATTAAA or
395 AATAAAA, or 3'-end peaks (if 3'-end-seq data is available). (C) Graphical illustration of the
396 identified events. The illustration also highlights unannotated short 3'-UTR transcript identified
397 from this task. The vertical red lines show the corresponding cleavage sites.



398

399 **Figure 2.** Simulation experiment to assess the performance of APA-Scan and the baseline
400 methods (DaPars and APAtrap). (a) Results on the simulation experiment with 30 million (30M)
401 short reads. (b) Results on the simulation experiment with 50M short reads. The receiver
402 operating characteristic (ROC) curves, i.e., true positive rate against false positive rate, are
403 plotted.

404



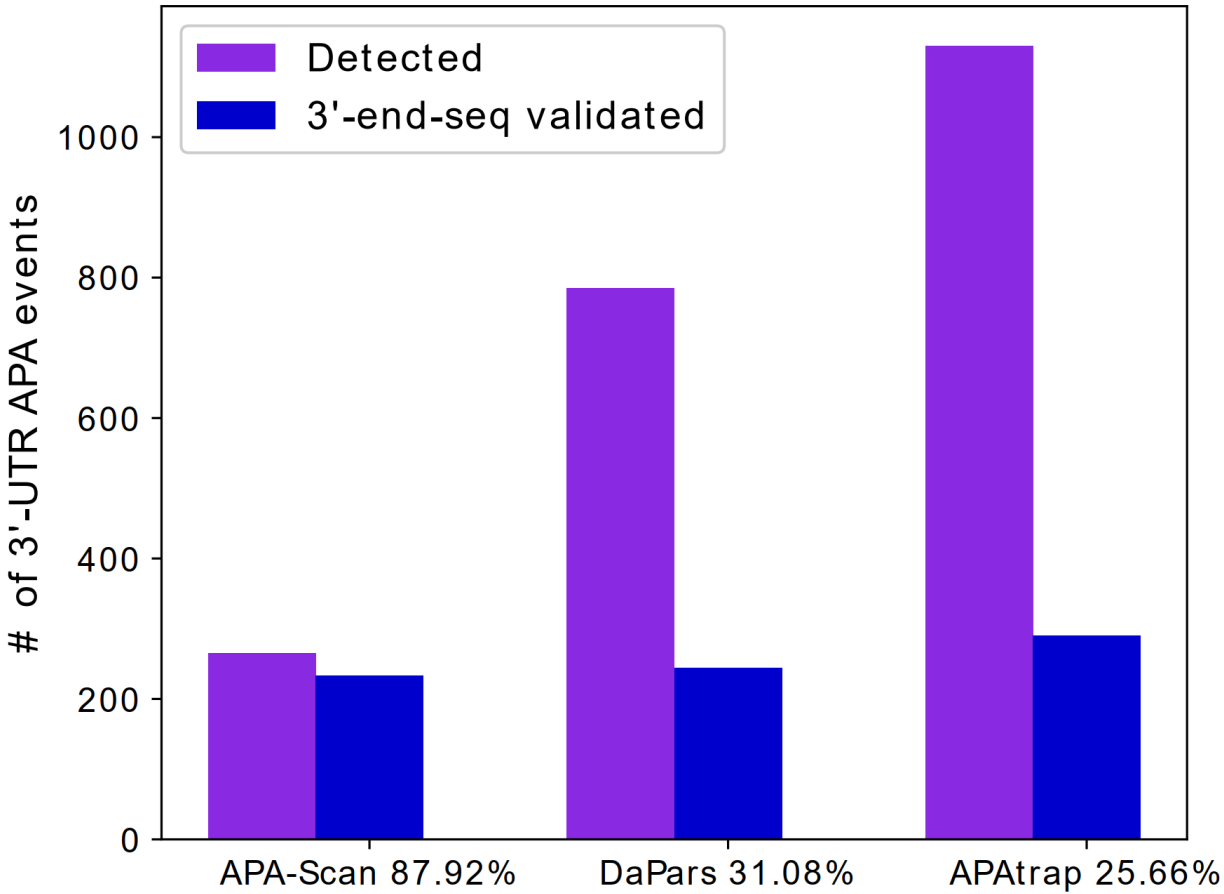
405

406

407

408

Figure 3. Simulation experiment to assess the performance of APA-Scan on different sequencing depths. The ROC curves for the results of different RNA-seq read depth are plotted.



409

410

411

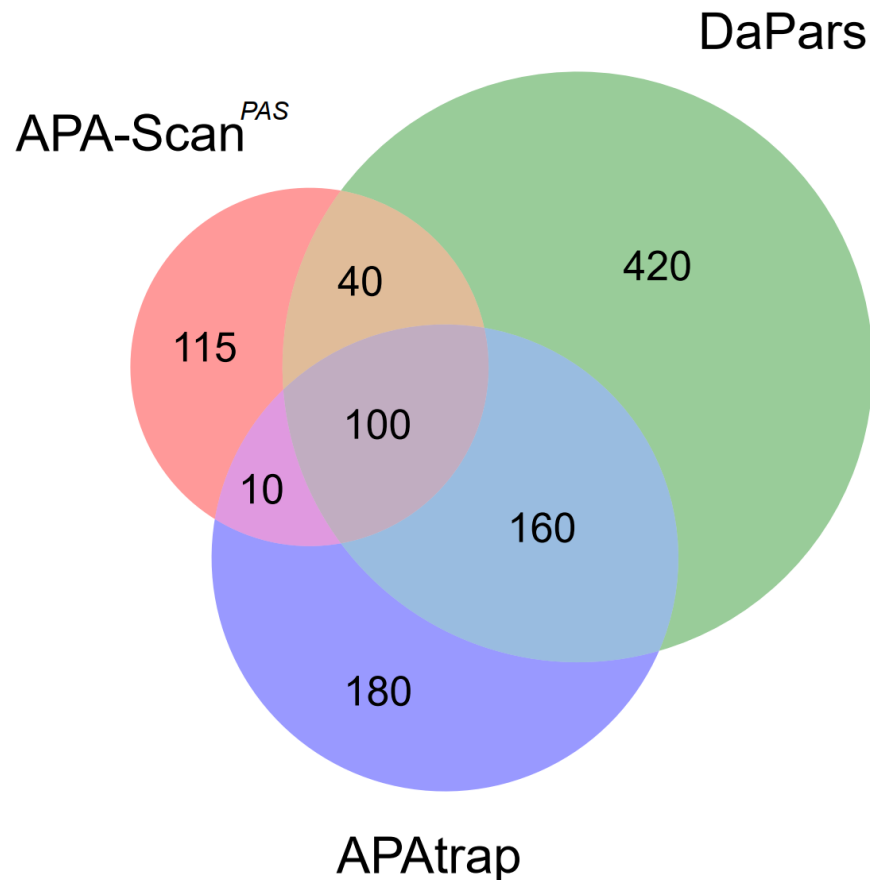
412

413

414

415

Figure 4. Evidence of polyadenylation sites supported by 3'-end-seq data for 3'-UTR APA events detected by different methods in MEFs samples. The number of events predicted by each method are shown in purple and the number of events validated by the signals in the 3'-end-seq data are shown in blue. The x-axis shows the percentage of the identified events is validated by 3'-end-seq.



416

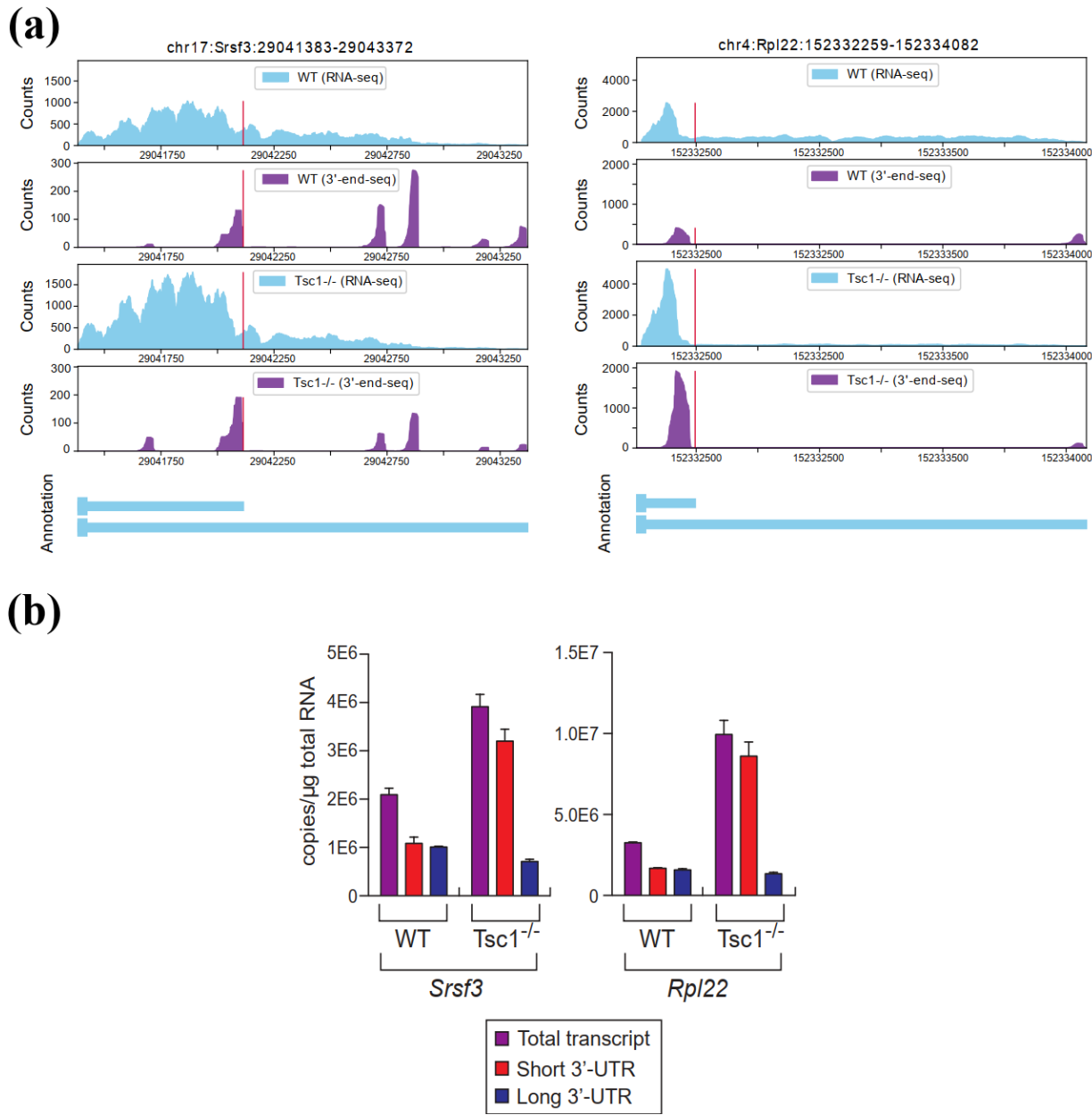
417

418

419

Figure 5. Venn diagram shows the overlapped genes with the 3'-UTR APA events identified by three methods (i.e., APA-Scan, DaPars and APAtrap) between two MEFs samples (WT vs $Tsc1^{-/-}$).

420



421

422

423

424

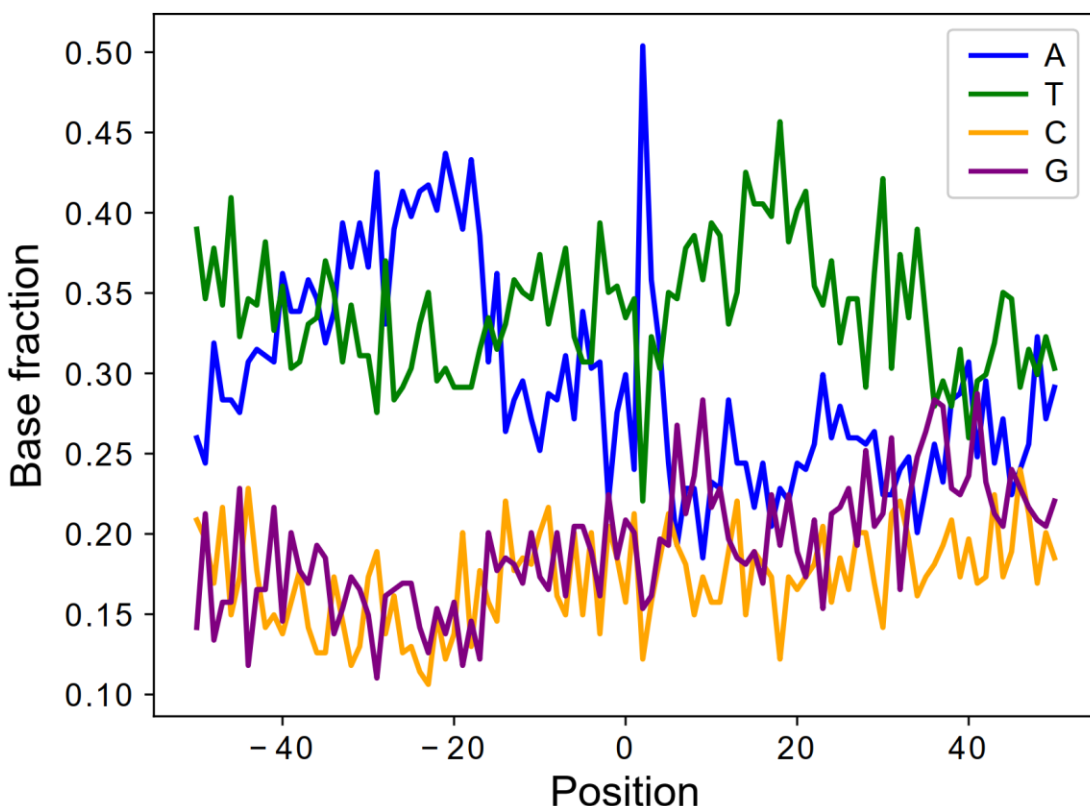
425

426

427

Figure 6. Experimental results: (a) RNA-seq and 3'-end-seq read coverage plots of the 3'-UTR in *Srsf3* and *Rpl22* gene in the two samples with isoform annotation. (b) The level of total, short 3'-UTR, and long 3'-UTR transcripts from *Srsf3* and *Rpl22* was measured by qPCR. Because it is not possible to design specific primers for the qPCR analysis of short 3'-UTR transcript, the amount of short 3'-UTR transcripts were calculated by subtracting the quantity of long 3'-UTR transcripts from total.

428



429

430 **Figure 7.** Nucleotide composition of the sequence surrounding the polyadenylation sites
431 identified by APA-Scan^{peaks} for MEFs samples. 50bp up and downstream region is plotted with
432 base sequences. x-axis denotes the position in the region, 0 is the location of the identified
433 polyadenylation site. y-axis shows the fraction of the nucleotides content at each position.

434

435

Table 1. Categorized overview of the technical parameters of APA-Scan

Categories	Types	Description
Input data	APA-Scan ^{peaks}	Both 3'-end-seq and RNA-seq data are provided
	APA-Scan ^{PAS}	Only RNA-seq data is provided
Mode	Default	Search for shorter 3'-UTR APA events
	Extended	Search for longer 3'-UTR APA events
Reported list	Default	List the most significant cleavage site for each gene
	All	List all candidate cleavage sites for each gene

436

437

438

Table 2. Comparison among APA-Scan, DaPars and APAtrap on simulated RNA-seq data with two different sequencing depths (30 million reads and 50 million reads). AUC (the area under the ROC curve) score, sensitivity, specificity of the three methods are reported. The best results across the three methods are bold.

Reads	Method	AUC	Sensitivity	Specificity
	APA-Scan	0.94	0.83	0.95
30M	DaPars	0.65	0.33	0.58
	APATrap	0.73	0.57	0.90
	APA-Scan	0.94	0.83	0.95
50M	DaPars	0.68	0.41	0.71
	APATrap	0.75	0.63	0.91

442

443

444

Table 3. Number of events detected by APA-Scan, DaPars and APAtrap and validated by 3'-end-seq data for MEFs samples.

Method	Detected	Validated by 3'-end-seq	Ratio (%)
APA-Scan	265	233	87.92
DaPars	785	244	31.08
APATrap	1130	290	25.66

446

447

448 **Table 4.** CPU time of APA-Scan, DaPars and APAtrap on two MEFs samples (WT vs $Tsc1^{-/-}$).

APA-Scan	DaPars	APAtrap
48 mins	21 hours	36 mins

449

450

451 **Additional Files**

452 **Additional file 1**

453 Figure S1; Figure S2; The command lines used for running the baseline methods; Parameters to
454 run flux-simulator; qPCR analysis and primer sequences.

455 **Additional file 2**

456 User's manual of APA-Scan

457

458

Supplementary

459

1 Running the baselines

460

1.1 DaPars

461

Inputs:

462

- BED files. Flux-simulator simulated three fastq files for three replicates in each condition. Using SAMtools (v0.1.8), read coverage files for each chromosome are generated in BAM format from the fastq files. Six bedgraph files in two conditions are generated from the BAM files using BEDtools.
- Gene annotation in .bed format: mm10_Refseq.bed
- Configuration file: configure.txt

466

467

```
Annotated_3UTR=mm10_Refseq_extracted_3UTR.bed
Group1_Tophat_aligned_Wig = case_1.bedgraph, case_2.bedgraph, case_3.bedgraph
Group2_Tophat_aligned_Wig = control_1.bedgraph, control_2.bedgraph,
control_3.bedgraph
Output_directory = DaPars_out/
Output_result_file = Dapars_out
Num_least_in_group1 = 1
Num_least_in_group2 = 1
Coverage_cutoff = 30
FDR_cutoff = 0.05
PDUI_cutoff = 0.1
Fold_change_cutoff = 0.59
```

468

Command 1:

```
python DaPars_Extract_Anno.py -b mm10_Refseq.bed
-s mm10_Refseq_id.txt -o mm10_Refseq_extracted_3UTR.bed
```

469

Command 2:

```
python DaPars_main.py configure.txt
```

470

471

1.2 APAtrap

472

Inputs:

473

474

- BED files. Flux-simulator simulated three fastq files for three replicates in each condition. Using SAMtools (v0.1.8), read coverage files for each chromosome are

475

476

477

478 generated in BAM format from the fastq files. Six bedgraph files in two
479 conditions are generated from the BAM files using BEDtools.

480 • Gene annotation in .bed format: mm10_Refseq.bed

481 **Command 1:**

482 identifyDistal3UTR -i A1.bedgraph A2.bedgraph A3.bedgraph B1.bedgraph B2.bedgraph
483 B3.bedgraph -m mm10_Refseq.bed -o mm10.utr.bed

484 **Command 2:**

485 predictAPA -i A1.bedgraph, A2.bedgraph, A3.bedgraph B1.bedgraph, B2.bedgraph,
486 B3.bedgraph -g 2 -n 3 3 -u mm10.utr.bed -o APA_output.txt

487 **Command 3:**

488 deAPA('APA_output.txt', 'APA_output.stat.txt', 1, 2, 1, 1, 20)

491 **2 Parameters to run flux-simulator (30 million reads)**

Parameters	Value	Description
REF_FILE_NAME	mm10.refGene.gtf	GTF reference annotation
GEN_DIR	Genome_mm10	Genomic sequences directory
NB_MOLECULES	8000000	Number of RNA molecules
TSS_MEAN	100	
POLYA_SCALE	100	Transcript modification parameters
POLYA_SHAPE	2	
FRAG_SUBSTRATE	DNA	
FRAG_METHOD	NB	Library Preparation parameters
FRAG_NB_LAMBDA	575	
FRAG_NB_M	1	
RTRANSCRIPTION	YES	Switch on reverse transcription
PCR_DISTRIBUTION	none	
GC_MEAN	NaN	Amplification parameters
GC_SD	NaN	
PCR_PROBABILITY	0.1	
FILTERING	YES	Switches size selection On
UNIQUE_IDS	TRUE	Create Unique Read Identifiers for paired-end
READ_NUMBER	30000000	Number of reads
READ_LENGTH	76	Length of each read
PAIRED_END	YES	Paired end reads

Parameters	Value	Description
FASTA	YES	Generate Fasta file
ERR_FILE	76	Error model for length 76

493

494

495

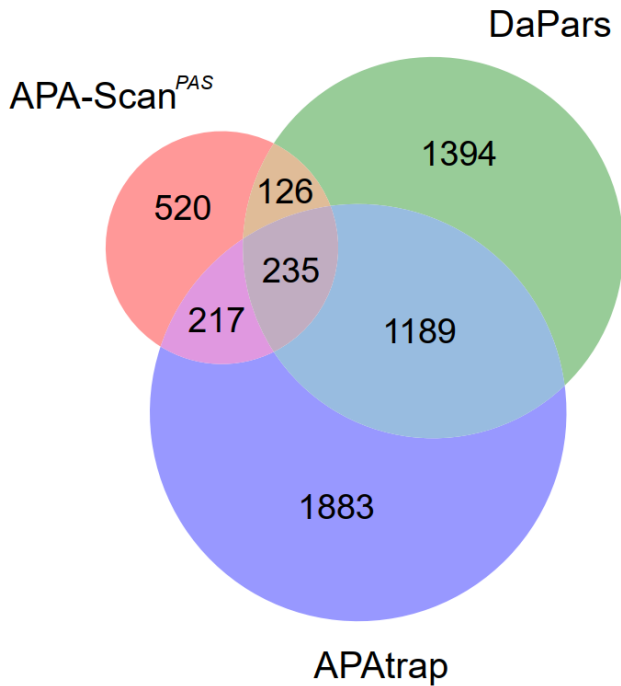
3 Realtime quantitative PCR (RT-qPCR) analysis and primer sequences

496 Total RNAs from TSC1 WT or TSC1-/ MEF cells were isolated by Trizol method according
497 to manufacturer's protocol ([https://assets.thermofisher.com/TFS-
498 Assets/LSG/manuals/trizol_reagent.pdf](https://assets.thermofisher.com/TFS-Assets/LSG/manuals/trizol_reagent.pdf)). Reverse transcription reaction using Oligo-d(T)
499 priming and NxGen M-MuLV Reverse transcriptase (Lucigen) was carried out according to
500 the manufacturer's protocol ([https://www.lucigen.com/docs/manuals/MA115-M-
501 MuLV.pdf](https://www.lucigen.com/docs/manuals/MA115-M-MuLV.pdf)). SYBR Green was used to detect and quantitate the PCR products in real-time
502 reactions. Quantitation of the real-time PCR results was done using standard curve method
503 for accuracy and reliability of the analysis. The primer sequences used to measure the RSI for
504 each transcript are as follows:

505 mRpl22 Total forward 5'-AAGTTCAC CCTGGACTGC AC-3'
506 mRpl22 Total reverse 5'-GTGATCTT GCTCTGCTG CG-3'
507 mRPL22 Long Forward 5'-TGGGCATC TGGGCTTTA GG-3'
508 mRPL22 Long reverse 5'-GCTTGTGCA GACTTGCTCA-3'
509 mSRSF3 Total forward 5'- GCTGCCGTGTAAGAGTGGAA-3'
510 mSRSF3 Total reverse 5'- AGGACTCCTCCTGCGGTAAT-3'
511 mSRSF3 Long forward 5'- TGCAACAGTCTGTGGCTTA-3'
512 mSRSF3 Long reverse 5'-TGCAATGGCTTACATAGACC-3'

513

4 Venn diagram for BT549 mock vs BT549 Torin1 treated



514

515
516

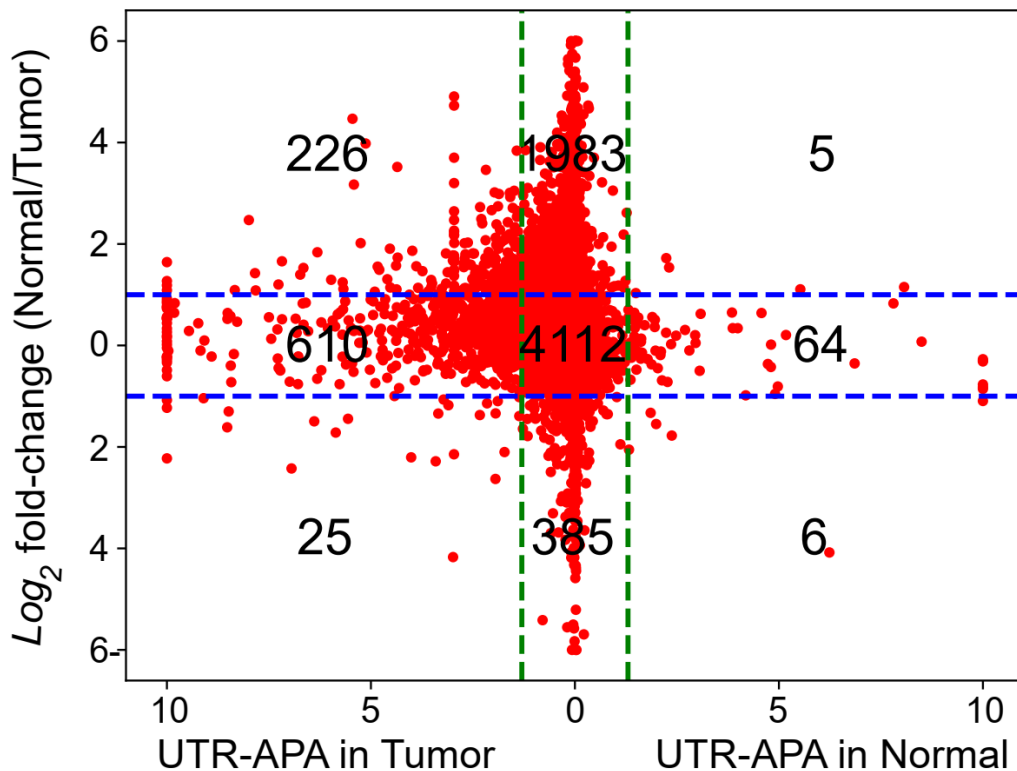
Figure S1: Venn diagram shows the overlapped genes with the 3'-UTR APA events identified by three methods between two breast cancer cell lines (BT549 mock vs BT549 Torin1 treated).

517

5 Experimental results with TCGA BRCA samples

518
519
520
521
522
523
524
525
526
527
528
529
530

One pair of TCGA breast cancer normal and tumor samples were selected and ran through APA-Scan for the detection of 3'-UTR APA. A total of 1266 APA events were detected between the two samples, whereas 1170 (92%) significant APA events were identified in tumor and 96 (8%) significant APA events were found in normal tissue sample. To inspect the correlation between 3'-UTR APA events and the gene expression profiles, we did the differential gene expression analysis and identified the genes in both tumor and normal samples. The result is illustrated in Figure 1. In the scatter plot, the y-axis denotes the Log_2 fold-change in the differential gene expression analysis and the x-axis shows the significance of UTR-APA ($\text{Log}_{10} p\text{-value}$). The left three sections and the right three sections show the 3'-UTR truncated genes in tumor and normal sample, respectively. The top three sections and the bottom three sections represent the up-regulated and down-regulated genes in normal tissue over tumor sample. This plot leads us to the observation that majority (>72%) of the 3'-UTR APA genes are not differentially expressed.



531
532
533
534
535
536
537
538

Figure S2: Scatter plot of APA and differentially expressed genes for TCGA tumor (TCGA-BH-A0BQ-01A) vs. matched normal tissue (TCGA-BH-A0BQ-11A) sample. Red dots represent individual gene in the analysis. Horizontal blue-dashed lines represent the cutoff values for two-fold changes in differential gene expression. Vertical green-dashed lines represent the cutoff values for $\log_{10}(p\text{-value})$ of 3'-UTR APA determined by the Chi-squared test.

539

APA-Scan User Manual

540

1 About

541
542
543
544
545

APA-Scan is a computational tool which can detect and visualize genome-wide 3'-UTR APA events. APA-Scan integrates both 3'-end-seq (an RNA-seq method with a specific enrichment of 3'-ends of mRNA) data and the location information of predicted canonical PAs with RNA-seq data to improve the quantitative definition of genome-wide UTR-APA events. It is also advantageous in producing high quality plots of the user defined events.

546

2 Download

547
548

APA-Scan is downloadable directly from <https://github.com/compbiolabucf/APA-Scan>. Users need to have python (version 3.0 or higher) installed in their machine to run APA-Scan.

549

3 Required Softwares

550

1. Python (version 3.0 or higher)
2. Samtools 0.1.8* [This specific version]

552

Required python packages

553

1. Pandas: \$ pip install pandas
2. Bio: \$ pip install biopython
3. Scipy: \$ pip install scipy
4. Numpy: \$ pip install numpy
5. Peakutils: \$ pip install PeakUtils

558

4 Run APA-Scan

559
560
561
562

APA-Scan can handle both human and mouse data for detecting potential APA truncation sites. The tool is designed to follow the format of Refseq annotation and genome file from UCSC Genome Browser. Users need to have the following two files in the parent directory in order to run APA-Scan:

563

1. Refseq annotation (.txt format)
2. Genome fasta file (downloaded from UCSC genome browser)

565

4.1 Required files

566
567

APA-Scan has two python scripts: **APA-Scan.py**, **Make-Plots.py**
And 1 configuration file: **configuration.ini**

568 The configuration file allows the user to specify the directories of the input samples, the species
569 to be analyzed and the directory where all output files will be stored.

570 APA-Scan supports the analysis of multiple samples that belong to two different groups- all
571 BAM files inside the input1 directory will be considered as part of the first group, and all BAM
572 files inside the input2 directory will be considered as part of the second group. It is required to
573 have at least one BAM file in each input directory.

574 **4.2 Running with parameters in the configuration.ini file**

575 (* refers to a mandatory field)

species*:	Species name (human/mouse)
input1* :	Directory containing the first group of samples with RNA-seq data [must be a folder name without ‘/’ at the end]
input2* :	Directory containing the second group of samples with RNA-seq data[must be a folder name without ‘/’ at the end]
pas1* :	Directory containing the first group of samples with 3’-end-seq data [must be a folder name without ‘/’ at the end]. Default is NULL
pas2* :	Directory containing the second group of samples with 3’-end-seq data [must be a folder name without ‘/’ at the end]. Default is NULL
extended* :	APA-Scan will run on ‘Extended 3UTR’ mode and it will search for APA sites upto 10kb downstream of the annotated transcript. Value: yes or no
All* :	If selected ‘yes’, APA-Scan will report all the candidate cleavage sites of a gene, whether they are significant or not. Otherwise, APA-Scan will report the most significant event for each gene [default]. Value: yes or no
annotation*	RefSeq annotation file, downloaded from UCSC Genome Browser, in .txt format
genome*	Genome fasta file, in .fa format
output_dir :	Output directory for writing the results. [optional]

576

577

578

An example of the coniguration.ini file is provided below:

```
[INPUT_RNAseq]
# Input folder names
# All samples(names like sample1_1.bam, sample1_2.bam....) in group1 must be inside of one folder
# All samples(names like sample1_1.bam, sample2_2.bam....) in group2 must be inside of one folder
input1 = /home/input/Group1
input2 = /home/input/Group2

[INPUT_PASseq]
# All samples(names like sample1_1.bam, sample1_2.bam....) in group1 must be inside of one folder
# All samples(names like sample1_1.bam, sample2_2.bam....) in group2 must be inside of one folder
# Default is NULL
pas1 = NULL
pas2 = NULL

[ANNOTATION]
# Put annotation and genome information
annotation = annotation.txt
genome = genome.fa

[Extended_3UTR]
# Run APA-Scan on 'Extended-3UTR' mode
# Value: yes/no. Default is no
extended = no

[All_events]
All = no

[OUTPUT_FOLDER]
output_dir = /home/output dirname
```

579

580

581 Once the parameters have been specified in the configuration file, the user will open a terminal
582 and enter the following command to run APA-Scan:

583

\$ python3 APA-Scan.py

584

585

586

587

588

589

APA-Scan.py will generate several intermediary files in the output directory. After computing the significance of the association between the two groups of samples, the final results will be written in the file named **Group1_Vs_Group2.csv**. The following image shows some of the generated fields in Group1_Vs_Group2.csv:

Chrom	Gene Name	Strand	Start	End	Position	p-value	Ratio Difference	Absolute ratio difference
chr19	RPL13A	+	49491728	49492307	49491826	1.92E-42	-0.065610766	0.065610766
chr10	VIM	+	17237229	17237597	17237318	4.61E-31	0.028446051	0.028446051
chr17	RPL26	-	8377515	8377692	8377564	2.98E-26	-0.04344075	0.04344075
chr5	STC2	-	173314722	173318249	173317376	2.33E-22	0.112542951	0.112542951
chr17	RPL19	+	39204524	39204730	39204650	1.03E-21	-0.049312569	0.049312569
chr13	CDC16	+	114272183	114272726	114272209	4.05E-17	-0.195062219	0.195062219
chr7	HNRNPA2B1	-	26189935	26192577	26191861	5.11E-16	-0.061955041	0.061955041
chr9	RABL6	+	136833719	136834476	136834327	5.68E-15	-0.30708408	0.30708408
chrX	RPS4X	-	72272602	72272772	72272628	2.08E-14	0.041582181	0.041582181
chr1	STMN1	-	25900115	25901087	25900534	2.9E-14	0.043951567	0.043951567
chr17	RPAIN	+	5432541	5433020	5432863	3.79E-14	0.061525048	0.061525048
chr6	SOD2	-	159679063	159682638	159682113	8.77E-14	-0.076980538	0.076980538
chr11	CCDC84	+	119015537	119015792	119015726	2.19E-12	-0.057536734	0.057536734
chr1	SYNC	-	32679905	32681860	32680315	4.57E-12	0.095614951	0.095614951
chr1	RPS8	+	44778575	44778740	44778687	1.21E-11	0.037494068	0.037494068
chr8	SFRP1	-	41261956	41265489	41265472	5.35E-11	-0.292512141	0.292512141
chr15	TPM1	+	63069869	63071914	63069945	5.54E-11	0.075237838	0.075237838
chr1	MEF2D	-	156463720	156467656	156467650	1.5E-10	-0.282933192	0.282933192
chr5	PHYKPL	-	178208473	178211970	178211572	3.28E-10	0.079757735	0.079757735
chr2	RPL37A	+	216501340	216501465	216501446	3.91E-10	0.019741659	0.019741659
chr12	PRIM1	-	56731579	56731734	56731638	8.48E-10	0.190879674	0.190879674
chr18	RCMC1	+	23531624	23531807	23531765	9.45E-10	-0.13019906	0.13019906

590

591 **5 Run Make-plots.py**

592 Make-plots.py also requires the same configuration file to run. It will use the input and output
593 directories listed in the configuration file and prepare a read coverage plot along with the 3'-
594 UTR annotation based on user defined region.

595
596 **python3 Make-plots.py**

597 After executing this command above for a few seconds, Make-plots.py will ask the user to insert
598 the region of interest in a specific format:

600
601 **Chrom:GeneName:RegionStart-RegionEnd**

602

603 **5.1 Make-plots.py parameter descriptions**

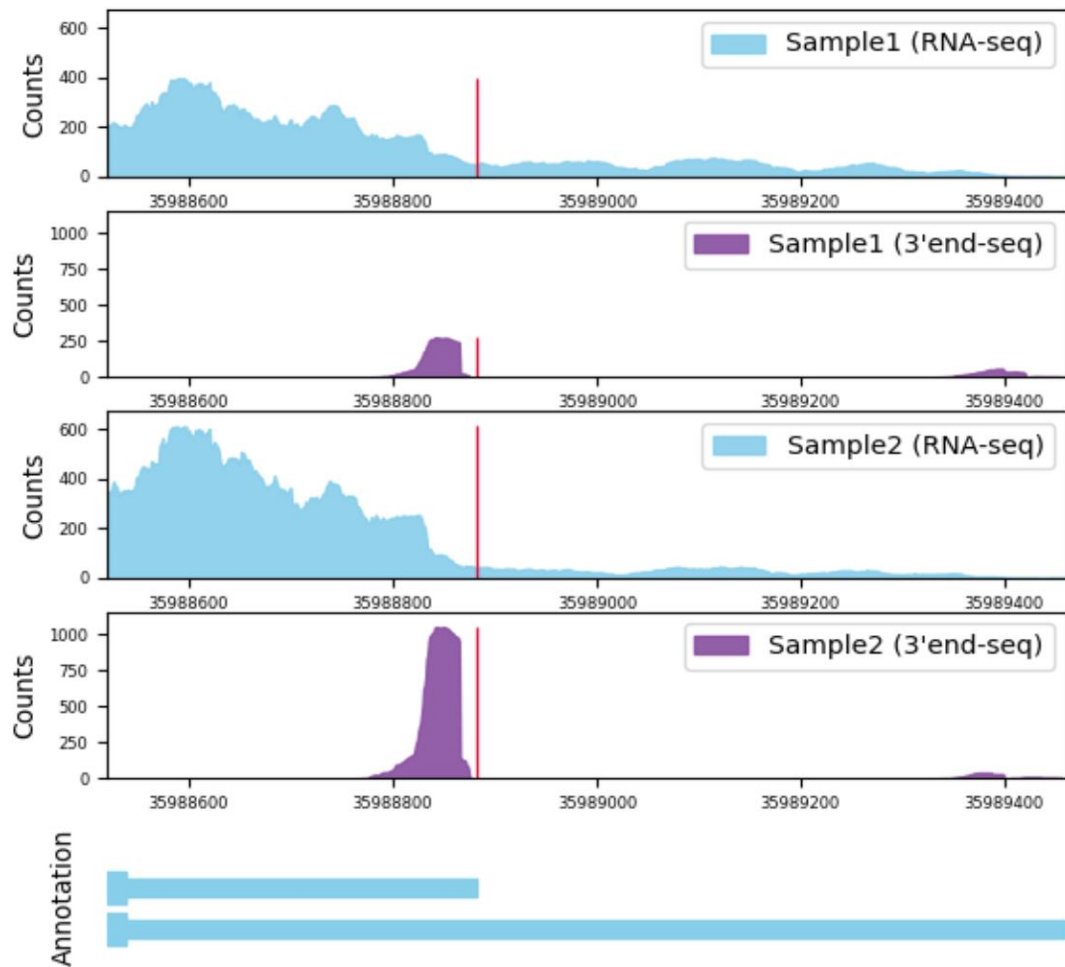
604

Chrom	Name of the chromosome
GeneName	Name of the gene
RegionStart	Starting position of the region
Region End	End position of the region

605
606 Example: **chr1:Tceb1:16641724-16643478**

607

608 Make-Plots.py will generate a visual representation of the results shown for each of the regions
609 entered. The plot will illustrate the most significant transcript cleavage site with a red vertical bar
610 on top of RNA-seq read data (and 3'end-seq if available). If the input parameters have 3'end-seq
611 information along with the RNA-seq, then it will generate plots for both cases (See figure
612 below). It will also show the UTR truncation point (annotated and unannotated) at the bottom
613 panel.



614
615
616
617

The first two subplots of the figure represent the read coverage of the two biological conditions. The bottom subplot shows the gene annotation and the exon information of that gene.